CARBON 50 (2012) 4476–4482

Available at www.sciencedirect.com

SciVerse ScienceDirect

journal homepage: www.elsevier.com/locate/carbon

A simple method to synthesize continuous large area nitrogen-doped graphene

Hui Gao [a,b,*], Li Song [c,f], Wenhua Guo [d], Liang Huang [a], Dezheng Yang [a], Fangcong Wang [a], Yalu Zuo [a], Xiaolong Fan [a], Zheng Liu [b], Wei Gao [e], Robert Vajtai [b], Ken Hackenberg [b], Pulickel M. Ajayan [b,e]

[a] Department of Materials Science, Lanzhou University, Lanzhou 730000, PR China
[b] Department of Mechanical Engineering and Materials Science, Rice University, Houston, TX 77005, USA
[c] Research Center for Exotic Nanocarbons, Shinshu University, Nagano 380-8553, Japan
[d] Department of Share Equipment Authority SEA, Rice University, Houston, TX 77005, USA
[e] Department of Chemistry, Rice University, Houston, TX 77005, USA
[f] National Synchrotron Radiation Laboratory, University of Science and Technology of China, Hefei 230026, PR China

ARTICLE INFO

Article history:
Received 2 November 2011
Accepted 13 May 2012
Available online 19 May 2012

ABSTRACT

Large area nitrogen (N)-doped graphene films were grown on copper foil by chemical vapor deposition. The as-grown films consisted of a single atomic layer that was continuous across the copper surface steps and grain boundaries, and could be easily transferred to a variety of substrates. N-doping was confirmed by X-ray photoelectron spectroscopy, Raman spectroscopy, and elemental mapping. N atoms were suggested to mainly form a "pyrrolic" nitrogen structure, and the doping level of N reached up to 3.4 at.%. The N-doped graphene exhibited an n-type behavior, and nitrogen doping would open a band gap in the graphene. This study presents use of a new liquid precursor to obtain large area, continuous and mostly single atom layer N-doped graphene films.

1. Introduction

Graphene consists of a single layer of sp^2-hybridized carbon atoms that are packed into a 2D honeycomb lattice. With its distinctive band structure and extraordinary electronic properties, graphene turns out to be quite promising in a plethora of applications [1,2]. Graphene is a zero-gap semiconductor, and its valence band intersects with the conduction band at K and K′ points in the reciprocal space. Therefore, graphene exhibits metallic conductivity even in the limit of nominally zero carrier concentration. The absence of a band gap in the intrinsic material renders it many applications in electronic devices [3]. Various approaches to improve the semiconducting properties of graphene have been proposed: doping with heteroatoms, chemical functionalization, confining the geometries of graphene to quantum dots or nanoribbons, and utilizing the interaction between graphene and particular substrates like SiC or SiO_2 [4–7]. Similar to other carbon materials like carbon nanotubes (CNTs), doping heteroatoms into graphene is a promising and feasible way to change its chemical composition and tailor its electronic band structure [8–10]. Doping can also be used to modify the local chemical activity of graphene for further chemical functionalization or modification [11,12]. Among all the available heteroatoms for doping, nitrogen (N) was chosen as a promising candidate due to its similar atomic size compared to carbon (C) atoms. Each N atom has five valence electrons, which occupy the 2s and

* *Corresponding author:* Fax: +86 931 8913554 (H. Gao).
E-mail address: hope@lzu.edu.cn (H. Gao).
0008-6223/$ - see front matter
http://dx.doi.org/10.1016/j.carbon.2012.05.026

2p atomic orbital and are available to form strong bonds with C atoms [13,14]. Incidentally, the metallic behavior was greatly enhanced in N-doped CNTs due to the additional lone pair of electrons from N atoms, and the introduced defects offered improvements in its sensitivity, catalytic activities, and biocompatibilities [15].

There have been four methods attempted to growing N-doped graphene: the first was to introduce a mixture of NH_3 and CH_4 into a chemical vapor deposition (CVD) system for the growth of the doped films [16,17]. Another was the post-treatment of exfoliated graphene or graphene oxide (GO) by high power electrical annealing in NH_3, NH_3 plasma, or NH_3 annealing after ion irradiation [18–20]. The third was the arc discharge between carbon electrodes in the presence of the compounds containing nitrogen such as pyridine [21]; And the last one was the growth of N-doped graphene from polymer and melamine [22]. Unfortunately most of these approaches have significant deficiencies and it is still a challenge to make intrinsically N-doped graphene [20]. For instance, the produced N-doped graphene films by exfoliating graphite or GO are limited by their small sizes (usually <1000 μm), making the technique non-scalable [18]. In the case of the N-doped graphene nanoribbons, it is very difficult to control the exact band gap level and doping is strongly related to the edge structure of the ribbon. Except in the case of the product from the post-treatment of single layered exfoliated graphene and polymer, multilayer films are very common in the above-mentioned methods and in the post-treatment case, the decomposition of NH_3 and rearrangement of N atoms into the honeycomb lattice require very high energy [16–18]. High vacuum is also needed in the process, and the difficulty to maintain this vacuum will give rise to the inhomogeneities in the gas pressure and thus doping compositions [23].

In this work, we developed a simple way to synthesize continuous single layered N-doped graphene with sizes on the order of centimeters by CVD technique. As a facile and inexpensive growth way, CVD is currently preferred route for preparing graphene in large scale [24–29]. Specifically, the doped graphene was grown using a novel liquid precursor (Dimethylformamide, DMF). DMF is one of the most inexpensive and commonly used organic solvents containing both N and C. N-doped graphene could also be synthesized by other nitrogen-containing organics such as pyridine or melamine [21,22]. Pyridine is a basic heterocyclic compounds, and C–N and C=N coexist in the structures. The flashing point of pyridine (21 °C) is much close to the room temperature. It is highly flammable and dangerous for the CVD growth. The melting point of melamine is too high, so it is difficult to directly synthesize the N-doped graphene via CVD technique. For DMF, the decomposition during CVD growth is easier than the above two organics because of its linear structure. In the CVD process, the N–C bond was broken at high temperature, and both atoms had a chance to rearrange into the matrix simultaneously, guaranteeing the homogeneity of N doping. A copper (Cu) substrate/catalytic layer was chosen for single layered graphene due to its lower carbon solubility and poorer carbon saturation compared with other metal substrates like nickel [30,31].

2. Experimental

The N-doped graphene was grown on a Cu foil substrate via a CVD reaction. The CVD chamber was pumped to 10^{-2} Torr, followed by a flow of H_2/Ar (volume ratio 1:5) at a pressure of ~10 Torr during heating. At 950 °C, the H_2/Ar flow was shut off and DMF vapor was introduced into the reaction chamber with a flow rate of 3 ml/h. After 3 min of growth, the chamber was cooled to 800 °C, and then to room temperature under an H_2/Ar atmosphere at the same pressure as before. The thickness of the graphene film could be controlled by changing the growth time. For comparison, the pristine graphene was also synthesized by CVD technique using hexane as the precursor as described in Ref. [23].

The as-prepared films on the Cu substrate were spin-coated with a thin layer of poly(methyl methacrylate) (PMMA). The Cu foil was then etched off in an aqueous solution of nitric acid. At this point, the freestanding PMMA-supported films could be transferred onto a variety of substrates such as quartz or SiO_2/Si. Finally the PMMA was removed by acetone, leaving behind the films for further investigations.

The samples were characterized by Raman spectroscopy (Renishaw in_By, with 514.5 nm laser), x-ray photoelectron spectroscopy (XPS) (PHI Quantera), scanning electron microscopy (SEM) (FEI Quanta 400 ESEM FEG), atomic force microscopy (AFM) (Digital instruments Nanoscope III A) and high resolution transmission electron microscopy (HRTEM) (JEM 2010).

The as-grown N-doped graphene films on SiO_2/Si substrate were used for the fabrication of a back-gated field-effect transistor (FETs) in large scale. Copper electrodes were plated onto the N-doped graphene films by the patterned thermal metal deposition. The N-doped graphene films act as the conducting channel between the source and drain electrodes. The channel length (L) and width (W) were about 450 μm and 1 cm. All of the reported electrical measurements were made at room temperature.

3. Results and discussion

Fig. 1a shows a photo of a typical N-doped graphene film (ca. 6 cm^2 in size) grown on a Cu foil. Fig. 1b shows a continuous and transparent film of about 2.3 cm in length on a quartz substrate after the transfer and dissolution of the PMMA (film indicated by the rectangle). Light interference on the SiO_2/Si substrate could be modulated by the graphene layers, so the change of color contrast in the optical images could indicate the variations of sample's thickness [32]. Fig. 1c shows the optical image of N-doped graphene, and the film appears to be quite uniform with only a small fraction of multilayers (<3%). Most area of the films (>97%) is monolayer, which will be further proved by Raman spectra. Fig. 1d and e show the SEM images of N-doped graphene grown on Cu foil and those of N-doped graphene transferred onto a SiO_2/Si substrate, respectively. The Cu grain boundaries are clearly visible, and the film is continuous across the surface steps and grain boundaries of Cu. The SEM image of N-doped graphene on SiO_2/Si shows a large and mostly flat surface. The wrinkles seen in Fig. 1e are associated with the thermal expansion

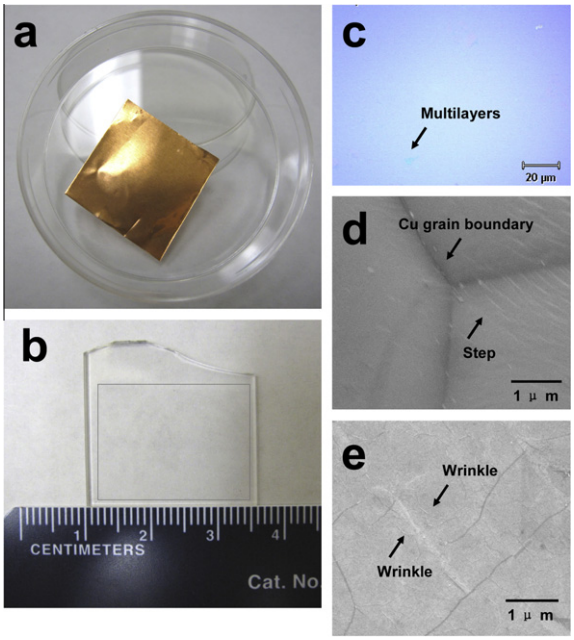

Fig. 1 – A typical digital photo of N-doped graphene film, (a) grown on Cu foil and (b) transferred onto quartz. (c) Optical image of N-doped graphene on SiO_2/Si substrate. SEM images of N-doped graphene film, (d) grown on Cu foil and (e) transferred onto SiO_2/Si.

coefficient differences between the substrate and N-doped graphene film.

We examined the Raman spectra of the samples to evaluate the graphitization in various parts of the as-grown films. As shown in Fig. 2, the typical Raman spectrum shows four features in the 1000–3000 cm^{-1} region, the D band (~1351.8 cm^{-1}), G band (~1591.6 cm^{-1}), D′ band (~1629.2 cm^{-1}) and 2D band (~2696.5 cm^{-1}). The D band, corresponding to the disorder-induced feature, only occurs in sp^2 carbon with defects. The higher intensity of D band indicates that N is doped into graphene, because the existence of heteroatoms has broken the symmetry of graphene lattice [22,32]. The D′ band emerging as a shoulder of the G band at a higher frequency is consid-

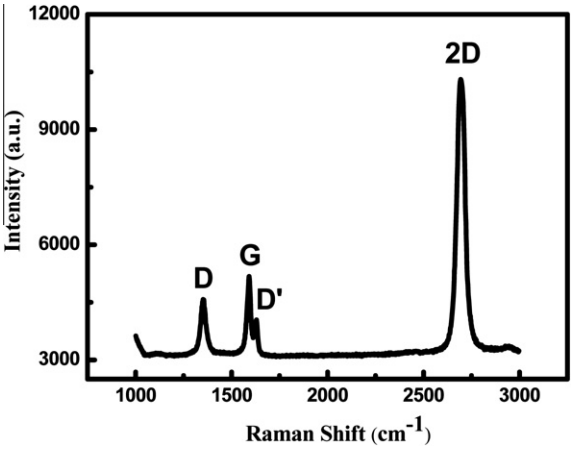

Fig. 2 – Raman spectrum of N-doped graphene with excitation wavelength of 514.5 nm.

ered another Raman feature induced by defects [33,34]. The I_D/I_G ratio for N-doped graphene is 0.87, representing the degree of disorder within the graphitic carbon. This is similar to results for N-doped CNTs [35]. The 2D band is sensitive to the doping as well as for determining the number of graphene layers. Upon doping, the I_{2D}/I_G ratio generally decreases with respect to that of pristine graphene. The ratio for our N-doped graphene is about 2, which is very close to that of N-doped graphene prepared from polymer and melamine, indicating the as-grown doped film is single layered [36].

The in-plane crystallite sizes (L_a) of the N-doped graphene is calculated using the following formula [37]:

$$L_a(nm) = (2.4 \times 10^{-10})\lambda^4 (I_D/I_G)^{-1}$$

where, λ is the Raman excitation wavelength, and I_D and I_G represent the relative intensity of D and G band. This gives an estimated crystallite size of about 19.3 nm.

To investigate the elemental composition as well as the chemical bonding environment of N atoms in N-doped graphene, XPS measurements were carried out to the synthesized films on SiO_2/Si substrate. As can be seen in Fig. 3a, the representative full spectrum shows N 1s peak at ca. 400 eV, confirming the incorporation of N atoms into the graphene lattice. It shows clear oxygen (O) 1s and C 1s peak at ca. 531.9 and 284.5 eV, respectively. The Si 2s and 2p peaks were also observed. The atomic percentage of N in the sample is about 3.4 at.%. The absence of Cu signal in the XPS spectrum validates that the Cu foil has been completely removed by the nitric acid solution. A high resolution XPS N 1s spectrum is given in Fig. 3b. The asymmetric N 1s peak can be decomposed into three peaks at 398.7, 399.9 and 401.6 eV, ordered from low to high binding energy. The small peaks at 398.7 and 401.6 eV correspond to pyridinic and quaternary (graphitic) structure of N bonds, and the high peak at 399.9 eV refers to pyrrolic type of N bond [19,38–40]. A schematic representation of three different bonding components of N atoms in the graphene lattice is shown in Fig. 4. In the pyridinic and pyrrolic cases, N is both bonded to two carbon atoms and donates one or two electrons to the aromatic π system. In the quaternary case, N replaces the carbon atom within the graphene layer and bonds to three carbon atoms. The pyrrolic structure is dominant based on the area ratio of the XPS peaks. The C 1s peak (Fig. 3c) can be decomposed into three apparent spectral components at 284.5, 286.1, and 287.7 eV. The main peak at 284.5 eV corresponds to the graphite-like sp^2 C, and the peak at 286.1 eV is attributed to C–OH bonds [19]. According to the previous reports, the peak corresponding to C–N bonds occurs at a binding energy of 287.5 ± 0.5 eV, which always overlaps with the C=O bond peak [41]. Thus, the N doping of graphite can reconfirmed by the 287.7 eV C–N peak of the C 1s high-resolution spectrum. The existence of bonding between C and O atoms is attributed to the oxidation on edge and defect positions or the O absorption onto the surface of N-doped graphene films [16,42].

It was reported that doping nitrogen into host graphene would increase the content of oxygen in graphene [19], and the phenomena were also observed in the N-doped CNTs [11]. We compared the high-resolution XPS spectra of O 1s of the pristine graphene and N-doped graphene (Fig. 3d and e). The highest peaks of both samples at 531.9 eV correspond to

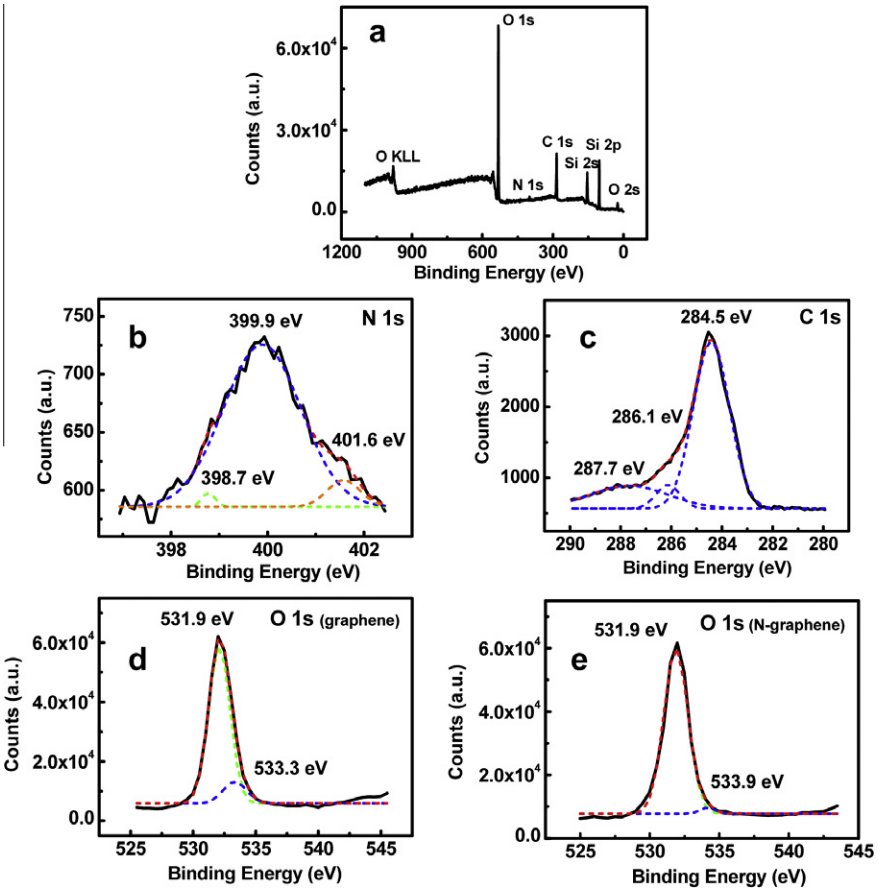

Fig. 3 – (a) XPS spectra of N-doped graphene on SiO_2/Si substrate. XPS high resolution spectrum of (b) N 1s spectrum and (c) C 1s spectrum in the N-doped graphene. O1s spectrum in the (d) pristine graphene and (e) N-doped graphene.

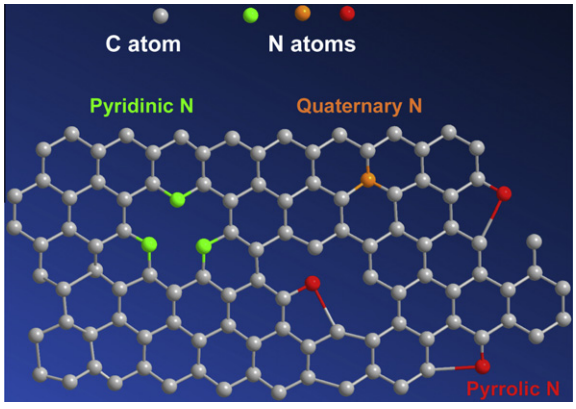

Fig. 4 – Schematic representation of N-doped graphene, the grey, red, green and orange spheres represent the C, pyrrolic N, pyridinic N and quaternary N atoms, respectively. (For interpretation of the references to colour in this figure legend, the reader is referred to the web version of this article.)

the bonding of Si–O, which arise from the SiO_2/Si substrate. The peak of C=O is overlaid with Si–O around the binding energy of 532.5 eV. And the peak at 533.9 eV is attributed to the bonding of C–OH [19]. Compared with the pristine graphene, the intensity of the peak in the range of 530.5–535.0 eV increased after N doping, indicating that the content of oxygen in the graphene has increased. The increasing O peak occurs mainly due to the organic precursor (DMF) containing C–O functionalities. Besides that, N doping introduces more defects according to the above Raman analysis, and the carbon atoms on the defects or edge plane could be easier oxidized to oxygen-containing functionalities, which also results in the increasing oxidized degree in the graphene [43].

Fig. 5a shows the low-magnification TEM image of N-doped graphene planar sheets. The sheet is flexible just like a large crumpled silk fabric. With Gatan image filter (GIF, a energy filtered imaging technique), we could map the elemental distribution of N in a selected area of the doped graphene film. The corresponding elemental mapping image (Fig. 5b) of Fig. 5a reconfirms that the N element is uniformly distributed (green color distribution) in the framework of graphene. Finding and observing an edge provides an accurate way to determine the number of layers [23]. The edges of the HRTEM image (Fig. 5c) indicate that the N-doped graphene is predominately single layered. AFM shows a smooth surface of the film with wrinkles due to its pliability in Fig. 6a. The film is highly continuous and uniform. The measured thickness for N-doped graphene is ~0.91 nm (Fig. 6b), which is close to that reported for single layer graphene on SiO_2 [23]. The aforemen-

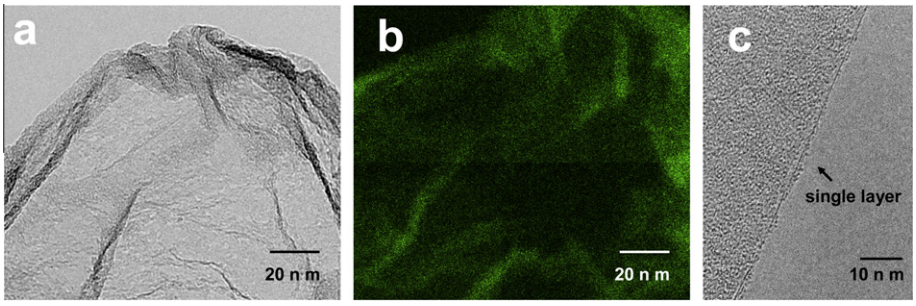

Fig. 5 – TEM analysis of N-doped graphene sheet. (a) Low-magnification TEM image. (b) The GIF elemental mapping image of N for (a). (c) High magnification TEM images of the edge of the N-doped graphene sheet.

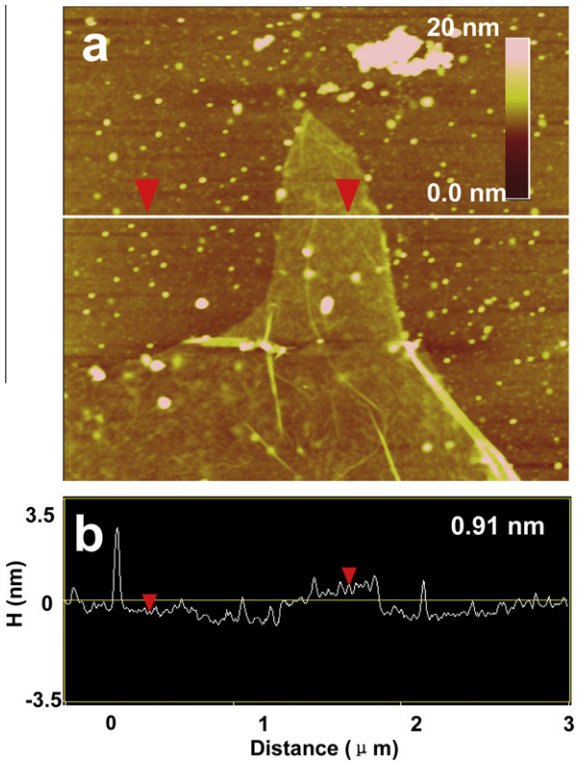

Fig. 6 – (a) AFM image of the N-doped graphene film. (b) The corresponding height analysis along the scanning horizontal lines marked in the AFM image.

tioned analyses of HRTEM and AFM images all agree with the analysis of the Raman spectrum, and the produced N-doped graphene is confirmed to be mostly single layered.

The FETs in large scale were fabricated. Fig. 7a shows a set of typical source-drain current (I_{ds}) vs the source-drain voltage (V_{ds}) at different gate voltage (V_g) for the N-doped graphene, and the transfer curve (at a fixed V_{ds} of 1.0 V) is shown in Fig. 7b. It is well known that pristine graphene shows good conductivity and linear I_{ds}–V_{ds} behavior. The typical sheet resistance and the mobilities are in about 100–300 Ω/o and 300–1200 cm^2/Vs for CVD grown pristine graphene [17,23]. In our investigation, the sheet resistance of N-doped graphene is in the range of 14-34 kΩ/o, and the mobilities are in about 310–630 cm^2/Vs according to the equation described by ref. [17]. Nitrogen doping breaks the symmetry of the graphene's lattice, and the introduced N atoms as well as the defects would behave as scattering centers, which suppress the mobilities and decrease the conductivity [14]. Similar to CNTs, the mobility of graphene would depend on the doping level, the number of removed C atoms and the defects in the lattice. For our N-doped graphene, the mobility is higher than the values (200–450 cm^2/Vs) reported for the previous reported N-doped graphene by CVD technique [17], which could be attributed to the lower N doping concentration in our sample (3.4 at%). As shown in Fig. 7b, I_{ds} increases with increasing V_g, indicating an n-type semiconductor behavior.

The inset of Fig. 7b shows the presumed band structure of the N-doped graphene. According to the previous theoretic calculation for N-doped CNTs, the nitrogen is energetically favorable for the site of pentagon ring but not for the heptagon ring [44]. And in our investigation, the N in the site of pentagon is predominant by XPS analysis. The band gap will be opened between the valence and conduction bands by the doping of N. The exact value of band gap would depend on

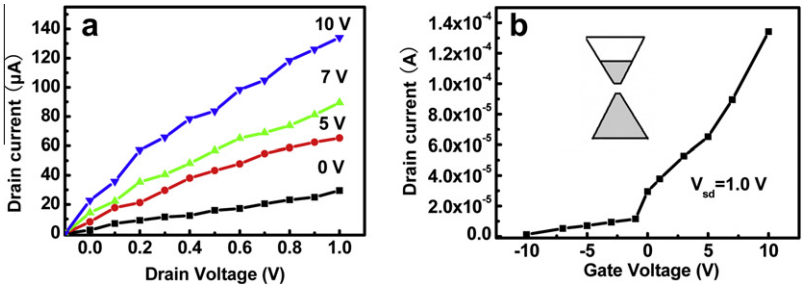

Fig. 7 – Output (a) and transfer (b) characteristics of the N-doped graphene.

the orientation of the pentagon and the site of carbon atoms replaced by N [45]. The pentagon N can introduce strong electron donor states near F_m and the as prepared N-doped graphene shows an n-type behavior, as discussed above.

4. Conclusion

We have demonstrated a one-step method for the growth of large-area, continuous, uniform and single layered N-doped graphene with DMF as the liquid precursor. Nitrogen doping along with the rearrangement of carbon atoms into a graphene lattice could be simultaneously realized in the CVD process, and the produced film could be transferred onto a variety of substrates. The as-synthesized N-doped graphene exhibits typical n-type semiconductor behavior, and N doping would modify the electrical structure of graphene. The study provides an elegant and cost effective method for synthesizing high quality nitrogen doped graphene.

Acknowledgements

H. Gao acknowledges support of Prof. Ajayan's Laboratory. This work was also supported by the Fundamental Research Funds for the Central Universities (lzujbky-2011-52) and the Key Laboratory of Materials for High-Power Laser Shanghai Institute of Optics and Fine Mechanics. L. Song thanks the support from Exotic Nanocarbons, Japan Regional Innovation Strategy Program by Excellence, JST.

REFERENCES

[1] Novoselov KS, Geim AK, Morozov SV, Jiang D, Zhang Y, Dubonos SV, et al. Electric field effect in atomically thin carbon films. Science 2004;306:666–9.
[2] Li XL, Zhang GY, Bai XD, Sun XM, Wang XR, Wang E, et al. Highly conducting graphene sheets and langmuir-Blodgett films. Nat Nanotechnol 2008;3:538–42.
[3] Geim AK, Novoselov KS. The rise of graphene. Nat Mater 2007;6:183–91.
[4] Pablo A. Denis, Band gap opening of monolayer and bilayer graphene doped with aluminium, silicion, phosphorus, and sulfur. Chem Phys Lett 2010;492:251–7.
[5] Choi J, Kim K-J, Kim B, Lee H, Kim S. Covalent functionalization of epitaxial graphene by azidotrimethylsilane. J Phys Chem C 2009;113:9433–5.
[6] Shemella P, Nayak SK. Electronic structure and band-gap modulation of graphene via substrate surface chemistry. Appl Phys Lett 2009;94:0321011–321013.
[7] Novoselov K. Graphene mind the gap. Nat Mater 2007;6:720–1.
[8] Duclaux L. Review of the doping of carbon nanotubes (multiwalled and single-walled). Carbon 2002;40:1751–64.
[9] Hsu WK, Nakajima T. Electrically conducting boron-doped multi-walled carbon nanotube bundles. Carbon 2002;40:462–7.
[10] Terrones H, Terrones M, Hemnádez E, Grobert N, Charlier J-C, Ajayan PM. New metallic allotrpes of planar and tubular carbon. Phys Rev Lett 2000;84:1716–9.
[11] Chen YG, Wang JJ, Liu H, Banis MN, Li RY, Sun XL, et al. Nitrogen doping effects on carbon nanotubes and the origin of the enhanced electrocatalytic activity of supported Pt for proton-exchange memebrane fuel cells. J Phys Chem C 2011;115:3769–76.
[12] Gong K, Du F, Xia Z, Durstock M, Dai L. Nitrogen-doped carbon nanotube arrays with high electrocatalytic activity for oxygen reduction. Science 2009;323:760–4.
[13] Lee SU, Belosludov RV, Mizuseki H, Kawazoe Y. Designing nanogadgetry for nanoelectronic devices with nitrogen-doped capped carbon nanotubes. Small 2009;5:1769–75.
[14] Xiao K, Liu YQ, Hu PA, Yu G, Sun YM, Zhu DB. N-type field-effect transistors made of an individual nitrogen-doped multiwalled carbon nanotube. J Am Chem Soc 2005;127:8614–7.
[15] Carrero-Sanchez JC, Ellias AL, Mancilla R, Arrellin G, Terrones H, Laclette JP, et al. Biocompatibility and toxicological studies of carbon nanotubes doped with nitrogen. Nano Lett 2006;6:1609–16.
[16] Qu LT, Liu Y, Baek J-B, Dai LM. Nitrogen-doped graphene as efficient metal-free electrocatalyst for oxygen reduction in fuel cells. Acs Nano 2010;4:1321–6.
[17] Wei DC, Liu YQ, Wang Y, Zhang HL, Huang LP, Yu G. Synthesis of N-doped graphene by chemical vapor deposition and its electrical properties. Nano Lett 2009;9:1752–8.
[18] Guo BD, Liu Q, Chen ED, Zhu HW, Fang LI, Gong JR. Controllable N-doping of graphene. Nano Lett 2010;10:4975–80.
[19] Wang Y, Shao YY, Matson DW, Li JH, Lin YH. Nitrogen-doped graphene and its application in electrochemical biosensing. Acs Nano 2010;4:1790–8.
[20] Wang XR, Li XL, Zhang Li, Yoon YK, Weber PK, Wang HL, et al. N doping of graphene through electrothermal reactions with ammonia. Science 2009;324:768–71.
[21] Panchakarla LS, Subrahmanyam KS, Saha SK, Govindaraj A, Krishnamurthy HR, Waghmare UV, et al. Synthesis, structure, and properties of boron- and nitrogen doped graphene. Adv Mater 2009;21:4726–30.
[22] Sun ZZ, Yan Z, Yao J, Beitler E, Zhu Y, Tour JM. Growth of graphene from solid carbon sources. Nature 2010;468:549–52.
[23] Srivastava A, Galande C, Ci LJ, Song L, Rai C, Jariwala D, et al. Novel liquid precursor-based facile synthesis of large-area continuous, single, and few-layer graphene films. Chem Mater 2010;22:3457–61.
[24] Reina A, Jia X, Ho J, Nezich D, Son H, Bulovic V, et al. Large area, few-layer graphene films on arbitrary substrates by chemical vapor deposition. Nano Lett 2009;9:30–5.
[25] Cai WW, Zhu YW, Li XS, Piner RD, Ruoff RS. Large area few-layer graphene/graphite films as transparent thin conducting electrodes. Appl Phys Lett 2009;95:1231151–3.
[26] Kim KS, Zhao Y, Jang H, Lee SY, Kim JM, Kim KS, et al. Large-scale pattern growth of graphene films for stretchable transparent electrodes. Nature 2009;457:706–10.
[27] Bae S, Kim H, Lee Y, Xu X, Park J-S, Zheng Y, et al. Roll-to-roll production of 30 inch graphene films for transparent electrodes. Nat Nanotechnol 2010;5:574–8.
[28] Gao L, Ren W, Zhao J, Ma L-P, Chen Z, Cheng H-M. Efficient growth of high quality graphene films on Cu foils by ambient pressure chemical vapor deposition. Appl Phys Lett 2010;97:1831091–3.
[29] Obraztsov AN. Chemical vapour deposition: making graphene on a large scale. Nat Nanotechnol 2009;4:212–3.
[30] Li XS, Cai WW, Colombo LG, Ruoff RS. Evolution of graphene growth on Ni and Cu by carbon isotope labeling. Nano Lett 2009;9:4268–72.
[31] Li XS, Cai WW, An JH, Kim S, Nah J, Yang DX, et al. Large-area synthesis of high-quality and uniform graphene films on copper foils. Science 2009;324:1312–4.
[32] Ferrari AC, Meyer JC, Scardaci V, Casiraghi C, Lazzeri M, Mauri F, et al. Raman spectrum of graphene and graphene layers. Phys Rev Lett 2006;97:1874011–4.

[33] Ci LJ, Song L, Jin CH, Jariwala D, Wu DX, Li YJ, et al. Atomic layer of hybridized boron nitride and graphene domains. Nat Mater 2010;9:430–5.
[34] Kudin KN, Ozbas B, Schniepp HC, Prud'homme RK, Aksay IA, Car R. Raman spectra of graphite oxide and functionalized graphene sheets. Nano Lett 2008;8:36–41.
[35] Xu EY, Wei JQ, Wang KL, Li Z, Gui XC, Jia Y, et al. Doped carbon nanotube array with a gradient of nitrogen concentration. Carbon 2010;48:3097–102.
[36] Das A, Pisana S, Chakraborty B, Piscanec S, Saha SK, Waghmare UV, et al. Monitoring dopants by Raman scattering in an electrochemically topgated graphene transistor. Nat Nanotechnol 2008;3:210–5.
[37] Cançado LG, Takai K, Enoki T, Endo M, Kim YA, Mizusaki H, et al. General equation for the determination of the crystallite size La of nanographite by Raman spectroscopy. Appl Phys Lett 2006;163106:88–90.
[38] Jansen RJJ, Vanbekkum H. XPS of nitrogen-containing functional-groups on activated carbon. Carbon 1995;33:1021–7.
[39] Nakayama Y, Soeda F, Ishitani A. XPS study of the carbon-fiber matrix interface. Carbon 1990;28:21–6.
[40] Wang XB, Liu YQ, Zhu DB, Zhang L, Ma HZ, Yao N, et al. Controllable growth, structure, and low field emission of well-aligned CN_x nanotubes. J Phys Chem B 2002;106:2186–90.
[41] Malitesta C, Losito I, Sabbatini L, Xambonin PG. New findings on polypyrrole chemical structure by XPS coupled to chemical derivatization labeling. J Electron Spectrosc Relat Phenom 1995;76:629–34.
[42] Collins PG, Bradley K, Ishigami M, Zettl A. Extreme oxygen sensitivity of electronic properties of carbon nanotubes. Science 2000;287:1804–8.
[43] Shalagina AE, Ismagilov ZR, Podyacheva OY, Kvon RI, Ushakov VA. Synthesis of nitrogen-containing carbon nanofibers by catalytic decomposition of ethylene/ammonia mixture. Carbon 2007;45:1808–20.
[44] Wei JW, Hu HF, Zeng H, Wang ZY, Wang L, Peng P. Effects of nitrogen in Stone-Wales defect on the electrical transport of carbon nanotube. Appl Phys Lett 2007;91:0921211–921213.
[45] Baskin A, Král P. Electronic structures of porous nanocarbons. Scientific Reports 2011;1:36.